Journal of Applied and Computational Mechanics, Vol. 2, No. 4, (2016), 222-229
DOI: 10.22055/JACM.2016.12542

Journal of
Applied and Computational Mechanics

Magnetic Field Effects on the Elastic Behavior of Polymeric Piezoelectric Cylinder Reinforced with CNTs

Ali Cheraghbak[1], **Abbas Loghman**[1]

[1] Faculty of Mechanical Engineering, University of Kashan, Kashan, Iran

Received November 14 2016; revised December 20 2016; accepted for publication December 30 2016.
Corresponding author: Ali Cheraghbak, ali.cheraghbeyk@gmail.com

Abstract

In the present study, the magnetic field effects of the elastic response of the polymeric piezoelectric cylinder reinforced with the carbon nanotubes (CNTs) are studied. The cylinder is subjected to an internal pressure, a constant electric potential difference at the inner and outer surfaces, and the thermal and magnetic fields. The Mori-Tanaka model is used for obtaining the equivalent material properties of the cylinder. The governing differential equation of the cylinder is derived and solved analytically based on the charge and equilibrium relations. The main purpose of this paper is to investigate the effects of the magnetic field on the stresses, the electric potential, and the radial displacement distributions of the polymeric piezoelectric cylinder. The presented results indicate that the existence of the magnetic field can reduce the stresses of the nanocomposite cylinder.

Keywords: Magnetic field; CNT; Piezoelectric cylinder; Mori-Tanak model; Electric filed.

1. Introduction

In recent years, there has been a resurgence of interest in the piezoelectricity which is motivated by advances in smart structures technology. The piezoelectric phenomenon has been exploited for decades. The classic piezoelectric devices include microphones and record players. More recent applications have focused on improving the existing devices and transforming them into ‘‘smart structures’’. For example, the piezoelectric actuators can be used to modify the shape of an airfoil to reduce transverse vortices or maintain a proper tension with overhead electrical wires on a locomotive pantograph. In addition to being used as actuators which respond to changes in an electric field by producing a mechanical strain, they can be used as sensors which respond to a mechanical strain by producing an electrical signal. One notable civil engineering application of the piezoelectric sensors is in the structural health monitoring. A change in the level of the strain will produce an electric charge and trigger the sensors in the structure.

For the homogeneous piezoelectric media, Ghorbanpour et al. [1] investigated the stress and the electric potential fields in the piezoelectric hollow spheres. Their results showed that an existing mechanical hoop stress distribution could be neutralized by a suitably applied electric field. Saadatfar and Razavi [2] analyzed the stress in a piezoelectric hollow cylinder with a thermal gradient. Moreover, an analytic solution to the axisymmetric problem of an infinitely long, radially polarized, and radially orthotropic piezoelectric hollow circular cylinder which rotates about its axis at constant angular velocity was developed by Galic and Horgan [3]. The analytical solution of a functionally graded piezothermoelastic hollow cylinder was presented by Chen and Shi [4]. They assumed that only the piezoelectric coefficient was varying quadratically in the radial direction, while the other material parameters were constant. Later, Babaei and chen [5] presented the analytical solution for a radially FGPM rotating hollow shaft. The same as [4] and [5], the elastic and piezoelectric constants were assumed to vary as a power function of the radius by Khoshgoftar et al. [6] who studied the behaviors of a thick-walled cylinder made of FGPM which was

subjected to the temperature gradient and inner and outer pressures. However, other inhomogeneity parameters such as the thermal conduction coefficient and the modulus of elasticity were neglected in [4] and [5].

With respect to the developmental works on the stress analysis of the cylinders, it should be noted that none of the researches mentioned above have considered the smart composites and their specific characteristics. The active control of the laminated cylindrical shells using the piezoelectric fiber reinforced composites was studied by Ray and Reddy [7] using the Mori-Tanaka model. However, the applied reinforced materials were CNTs which are not smart. Additionally, Bohm and Nogales [8] studied the thermal conduction behavior of the metal matrix composites reinforced with the polyhedral particles using the Mori–Tanaka method. The micromechanical modeling, which has the potential to take into account the electrical load, was used by Tan and Tong [9] for studying an imperfect textile composite. However, neither the matrix nor the reinforced material used in the composite which was employed in this work was smart. The agglomeration effect on the electro-magneto-thermo elastic response of a hollow piezoelectric circular cylinder reinforced with the carbon nanotubes (CNTs) was presented by Loghman and Cheraghbak [10].

In the present work, the magnetic field effects on the magneto-electro-thermo elastic behavior of a piezoelectric nanocomposite cylinder are considered. The cylinder is subjected to mechanical, magnetic, and thermal loads. Moreover, an electric potential difference is induced by the electrodes attached to the inner and outer surfaces of the cylinder. Finally, the stresses, the electric potential, and the displacement distributions of the piezoelectric cylinder are obtained using exact solution.

2. Mori-Tanaka Model

In this section, the effective modulus of the composite shell reinforced with CNTs is developed. Different methods are available to obtain the average properties of a composite [11]. Due to its simplicity and accuracy even at high volume fractions of the inclusions, the Mori-Tanaka method [11] is employed in this section. The CNTs content is assumed to be aligned and straight with a uniform dispersion in the polymer matrix. The matrix is assumed to be isotropic and elastic, compared with the Young's modulus E_m and the Poisson's ratio υ_m. The constitutive relations for a layer of the composite with the principal axes parallel to the r, θ, and z directions are [10]:

$$\begin{Bmatrix}\sigma_{11}\\ \sigma_{22}\\ \sigma_{33}\\ \sigma_{23}\\ \sigma_{13}\\ \sigma_{12}\end{Bmatrix}=\begin{bmatrix}k+m & l & k-m & 0 & 0 & 0\\ l & n & l & 0 & 0 & 0\\ k-m & l & k+m & 0 & 0 & 0\\ 0 & 0 & 0 & p & 0 & 0\\ 0 & 0 & 0 & 0 & m & 0\\ 0 & 0 & 0 & 0 & 0 & p\end{bmatrix}\begin{Bmatrix}\varepsilon_{11}\\ \varepsilon_{22}\\ \varepsilon_{33}\\ \gamma_{23}\\ \gamma_{13}\\ \gamma_{12}\end{Bmatrix} \tag{1}$$

where $\sigma_{ij}, \varepsilon_{ij}, \gamma_{ij}, k, m, n, l, p$ are the stress components, the strain components, and the stiffness coefficients, respectively. According to the Mori-Tanaka method, the stiffness coefficients are given by [10-12]:

$$\begin{aligned}
k &= \frac{E_m\{E_m c_m + 2k_r(1+\nu_m)[1+c_r(1-2\nu_m)]\}}{2(1+\nu_m)[E_m(1+c_r-2\nu_m)+2c_m k_r(1-\nu_m-2\nu_m^2)]}\\
l &= \frac{E_m\{c_m\nu_m[E_m+2k_r(1+\nu_m)]+2c_r l_r(1-\nu_m^2)]\}}{(1+\nu_m)[E_m(1+c_r-2\nu_m)+2c_m k_r(1-\nu_m-2\nu_m^2)]}\\
n &= \frac{E_m^2 c_m(1+c_r-c_m\nu_m)+2c_m c_r(k_r n_r - l_r^2)(1+\nu_m)^2(1-2\nu_m)}{(1+\nu_m)[E_m(1+c_r-2\nu_m)+2c_m k_r(1-\nu_m-2\nu_m^2)]}\\
&\quad + \frac{E_m[2c_m^2 k_r(1-\nu_m)+c_r n_r(1+c_r-2\nu_m)-4c_m l_r\nu_m]}{E_m(1+c_r-2\nu_m)+2c_m k_r(1-\nu_m-2\nu_m^2)}\\
p &= \frac{E_m[E_m c_m + 2p_r(1+\nu_m)(1+c_r)]}{2(1+\nu_m)[E_m(1+c_r)+2c_m p_r(1+\nu_m)]}\\
m &= \frac{E_m[E_m c_m + 2m_r(1+\nu_m)(3+c_r-4\nu_m)]}{2(1+\nu_m)\{E_m[c_m+4c_r(1-\nu_m)]+2c_m m_r(3-\nu_m-4\nu_m^2)\}}
\end{aligned} \tag{2}$$

where the subscripts m and r stand for matrix and reinforcement, respectively. C_m and C_r are the volume fractions of the matrix and CNTs, respectively, and k_r ، l_r ، n_r ، p_r , m_r are the Hills' elastic modulus for CNTs [10].

3. Governing equations

As presented in Fig. 1, the hollow circular piezoelectric cylinder is considered with the inner and outer radius of a and b, respectively, and is subjected to the axisymmetric thermo-mechanical and electrical loadings. The governing equations for a homogeneous anisotropic piezoelectric cylinder can be written as ([13]):

$$\begin{bmatrix}\sigma_{rr}\\ \sigma_{\theta\theta}\\ \sigma_{zz}\\ \tau_{\theta z}\\ \tau_{rz}\\ \tau_{r\theta}\end{bmatrix}=\begin{bmatrix}C_{11} & C_{12} & C_{13} & 0 & 0 & 0\\ C_{12} & C_{22} & C_{23} & 0 & 0 & 0\\ C_{13} & C_{23} & C_{33} & 0 & 0 & 0\\ 0 & 0 & 0 & C_{44} & 0 & 0\\ 0 & 0 & 0 & 0 & C_{55} & 0\\ 0 & 0 & 0 & 0 & 0 & C_{66}\end{bmatrix}\left(\begin{Bmatrix}\varepsilon_{rr}\\ \varepsilon_{\theta\theta}\\ \varepsilon_{zz}\\ 2\varepsilon_{\theta z}\\ 2\varepsilon_{rz}\\ 2\varepsilon_{r\theta}\end{Bmatrix}-\begin{Bmatrix}\alpha_{rr}\\ \alpha_{\theta\theta}\\ \alpha_{zz}\\ 0\\ 0\\ 0\end{Bmatrix}T\right)-\begin{bmatrix}e_{11} & 0 & 0\\ e_{12} & 0 & 0\\ e_{13} & 0 & 0\\ 0 & e_{24} & 0\\ 0 & 0 & e_{35}\\ 0 & 0 & 0\end{bmatrix}\begin{Bmatrix}E_{rr}\\ E_{\theta\theta}\\ E_{zz}\end{Bmatrix}, \tag{3}$$

$$\begin{bmatrix}D_{rr}\\ D_{\theta\theta}\\ D_{zz}\end{bmatrix}=\begin{bmatrix}e_{11} & e_{12} & e_{13} & 0 & 0 & 0\\ 0 & 0 & 0 & e_{24} & 0 & 0\\ 0 & 0 & 0 & 0 & e_{35} & 0\end{bmatrix}\left(\begin{Bmatrix}\varepsilon_{rr}\\ \varepsilon_{\theta\theta}\\ \varepsilon_{zz}\\ 2\varepsilon_{\theta z}\\ 2\varepsilon_{rz}\\ 2\varepsilon_{r\theta}\end{Bmatrix}-\begin{Bmatrix}\alpha_{rr}\\ \alpha_{\theta\theta}\\ \alpha_{zz}\\ 0\\ 0\\ 0\end{Bmatrix}T\right)+\begin{bmatrix}\in_{11} & 0 & 0\\ 0 & \in_{22} & 0\\ 0 & 0 & \in_{33}\end{bmatrix}\begin{Bmatrix}E_{rr}\\ E_{\theta\theta}\\ E_{zz}\end{Bmatrix}. \tag{4}$$

where ε_{ij} and σ_{ij} are the mechanical strain and the stress, respectively, c_{ijkl} is the elastic compliance, D_m is the component of the electric displacement (also referred to as charge density), E_m is the component of the electric field, e_{mi} is the piezoelectric module which relates the electrical and mechanical effects, and $\in_{mk}$ is the dielectric permittivity constant at the constant stress. It is also noted that the electric field E_m can be written in terms of the electric potential ϕ as:

$$E=-\nabla\phi. \tag{5}$$

In addition, the temperature distribution can be obtained as:

$$T(r)=F_1\ln(\mathrm{r})+\mathrm{F}_2, \tag{6}$$

where F_1 and F_2 are obtained from the thermal boundary conditions at the inner and outer surfaces.

The components of the displacement and the electric potential are assumed as:

$$\begin{aligned}u_r&=u(r),\\ u_z&=0,\\ u_\theta&=0,\\ \phi&=\phi(r).\end{aligned} \tag{7}$$

The equation of equilibrium and the Maxwell's equation for the free electric charge density ([11] and [14]) are written as:

$$\frac{\partial\sigma_{rr}}{\partial r}+\frac{\sigma_{rr}-\sigma_{\theta\theta}}{r}+f_z=0. \tag{8}$$

$$\frac{\partial D_{rr}}{\partial r}+\frac{D_{rr}}{r}=0. \tag{9}$$

where $\sigma_{ii}\ (i=r,\theta)$ is the stress tensor and D_{rr} is the radial electric displacement, respectively.

Furthermore, f_z is the Lorentz force which may be written as [15]:

$$f_z=\mu {H_z}^2\frac{\partial}{\partial r}\left(\frac{\partial u}{\partial r}+\frac{u}{r}\right) \tag{10}$$

The radial and circumferential strains and the relations between the electric field and the electric potential are therefore reduced to:

$$\varepsilon_{rr}=\frac{\partial u}{\partial r}, \tag{11}$$

$$\varepsilon_{\theta\theta}=\frac{u}{r}, \tag{12}$$

$$E_{rr}=-\frac{\partial\phi}{\partial r}. \tag{13}$$

The corresponding constitutive relations and the components of the radial electric displacement vector may be written as:

$$\sigma_{rr}=C_{11}\left(\varepsilon_{rr}-\alpha_{rr}T(r)\right)+C_{12}\left(\varepsilon_{\theta\theta}-\alpha_{\theta\theta}T(r)\right)-e_{11}E_{rr}, \tag{14}$$

$$\sigma_{\theta\theta}=C_{12}\left(\varepsilon_{rr}-\alpha_{rr}T(r)\right)+C_{22}\left(\varepsilon_{\theta\theta}-\alpha_{\theta\theta}T(r)\right)-e_{12}E_{rr}, \tag{15}$$

$$\sigma_{zz}=C_{13}\left(\varepsilon_{rr}-\alpha_{rr}T(r)\right)+C_{23}\left(\varepsilon_{\theta\theta}-\alpha_{\theta\theta}T(r)\right)-e_{13}E_{rr}, \tag{16}$$

$$D_{rr} = e_{11}\left(\varepsilon_{rr} - \alpha_{rr}T(r)\right) + e_{12}\left(\varepsilon_{\theta\theta} - \alpha_{\theta\theta}T(r)\right) + \in_{11} E_{rr}, \tag{17}$$

To develop the analytical solution, the following dimensionless quantities are introduced:

$$\sigma_r = \frac{\sigma_{rr}}{C_{22}}, \quad \sigma_\theta = \frac{\sigma_{\theta\theta}}{C_{22}}, \quad \sigma_z = \frac{\sigma_{zz}}{C_{22}}, \quad U = \frac{u}{a}, \quad \chi = \frac{r}{a}, \quad \beta = \frac{b}{a}, \tag{18}$$

$$\Phi = \frac{\phi}{\phi_0}, \ \phi_0 = a\sqrt{\frac{C_{22}}{\in_{11}}}, \quad \Psi_r = \frac{D_{rr}}{\sqrt{C_{22}\in_{11}}}, \quad C_1 = \frac{C_{11}}{C_{22}}, C_3 = \frac{C_{13}}{C_{22}}, C_4 = \frac{C_{33}}{C_{22}},$$

$$C_2 = \frac{C_{12}}{C_{22}}, \quad \Xi_1 = \frac{e_{11}}{\sqrt{C_{22}\in_{11}}}, \quad \Xi_2 = \frac{e_{12}}{\sqrt{C_{22}\in_{11}}}, \Xi_3 = \frac{e_{13}}{\sqrt{C_{22}\in_{11}}}, \overline{H}_Z = \frac{\mu H_z^{\ 2}}{C_{22}}$$

Using these dimensionless variables, the constitutive equations may be rewritten in the non-dimensional form as:

$$T(\chi) = F_1 \ln(\chi) + F_2, \tag{19}$$

$$\sigma_r = C_1\left(\frac{dU}{d\chi} - \alpha_{rr}\left(F_1\ln(\chi)+F_2\right)\right) + C_2\left(\frac{U}{\chi} - \alpha_{\theta\theta}\left(F_1\ln(\chi)+F_2\right)\right) + \Xi_1\frac{d\Phi}{d\chi}, \tag{20}$$

$$\sigma_\theta = C_2\left(\frac{dU}{d\chi} - \alpha_{rr}\left(F_1\ln(\chi)+F_2\right)\right) + \left(\frac{U}{\chi} - \alpha_{\theta\theta}\left(F_1\ln(\chi)+F_2\right)\right) + \Xi_2\frac{d\Phi}{d\chi}, \tag{21}$$

$$\sigma_z = C_3\left(\frac{dU}{d\chi} - \alpha_{rr}\left(F_1\ln(\chi)+F_2\right)\right) + C_4\left(\frac{U}{\chi} - \alpha_{\theta\theta}\left(F_1\ln(\chi)+F_2\right)\right) + \Xi_3\frac{d\Phi}{d\chi}, \tag{22}$$

$$\Psi_r = \Xi_1\left(\frac{dU}{d\chi} - \alpha_{rr}\left(F_1\ln(\chi)+F_2\right)\right) + \Xi_2\left(\frac{U}{\chi} - \alpha_{\theta\theta}\left(F_1\ln(\chi)+F_2\right)\right) - \frac{d\Phi}{d\chi}, \tag{23}$$

$$\frac{\partial\sigma_r}{\partial\chi} + \frac{\sigma_r - \sigma_\theta}{\chi} + \overline{H}_z \ \ \frac{\partial}{\partial\chi}\left(\frac{\partial U}{\partial\chi} + \frac{U}{\chi}\right) = 0. \tag{24}$$

$$\frac{\partial\Psi_r}{\partial\chi} + \frac{\Psi_r}{\chi} = 0. \tag{25}$$

The solution of Eq. (25) is $\Psi_r = F/\chi$ where F_3 is a constant. By substituting this equation into Eq. (23), we obtain:

$$\frac{d\Phi}{d\chi} = -\frac{F_3}{\chi} + \Xi_1\left(\frac{dU}{d\chi} - \alpha_{rr}\left(F_1\ln(\chi)+F_2\right)\right) + \Xi_2\left(\frac{U}{\chi} - \alpha_{\theta\theta}\left(F_1\ln(\chi)+F_2\right)\right). \tag{26}$$

Substituting Eq. (27) into Eqs. (20), (21), and (22) yields:

$$\sigma_r = \left(C_1+\Xi_1^2\right)\left(\frac{dU}{d\chi} - \alpha_{rr}\left(F_1\ln(\chi)+F_2\right)\right) + \left(C_2+\Xi_2\Xi_1\right)\left(\frac{U}{\chi} - \alpha_{\theta\theta}\left(F_1\ln(\chi)+F_2\right)\right) - F_3\Xi_1\chi^{-1}, \tag{27}$$

$$\sigma_\theta = \left(C_2+\Xi_1\Xi_2\right)\left(\frac{dU}{d\chi} - \alpha_{rr}\left(F_1\ln(\chi)+F_2\right)\right) + \left(1+\Xi_2^2\right)\left(\frac{U}{\chi} - \alpha_{\theta\theta}\left(F_1\ln(\chi)+F_2\right)\right) - F_3\Xi_2\chi^{-1}, \tag{28}$$

$$\sigma_z = \left(C_3+\Xi_1\Xi_2\right)\left(\frac{dU}{d\chi} - \alpha_{rr}\left(F_1\ln(\chi)+F_2\right)\right) + \left(C_4+\Xi_2^2\right)\left(\frac{U}{\chi} - \alpha_{\theta\theta}\left(F_1\ln(\chi)+F_2\right)\right) - F_3\Xi_4\chi^{-1}, \tag{29}$$

Finally, substituting Eqs. (27) and (28) into Eq. (24) yields the following non-homogeneous ordinary differential equation as:

$$\chi^2\frac{d^2U}{d\chi^2} + \chi L_1\frac{dU}{d\chi} + L_2U = -L_3\chi - L_4\chi\ln(\chi) - L_5, \tag{30}$$

where

$$L_1 = 1, \tag{31}$$

$$L_2 = \frac{-\overline{H}_z - \Xi_2^2 - 1}{C_1 + \Xi_1^2 + \overline{H}_z}, \tag{32}$$

$$L_3 = \frac{-F_2\left(\begin{matrix}C_2\alpha_\theta + C_2\alpha_r + C_1\alpha_r + \Xi_1^2\alpha_r - \\ \Xi_2^2\alpha_\theta - \alpha_\theta + \Xi_1\Xi_2\alpha_\theta - \Xi_1\Xi_2\alpha_r\end{matrix}\right) - F_1\left(\Xi_1^2\alpha_r + C_2\alpha_\theta + \Xi_1\Xi_2\alpha_\theta + C_1\alpha_r\right)}{C_1 + \Xi_1^2 + \overline{H}_z}, \tag{33}$$

$$L_4 = \frac{F_1\left(\alpha_\theta + \Xi_2^2\alpha_\theta - C_2\alpha_\theta + \Xi_1\Xi_2\alpha_r - C_1\alpha_r - \Xi_1^2\alpha_r - \Xi_1\Xi_2\alpha_\theta\right)}{C_1 + \Xi_1^2 + \overline{H}_z}, \tag{34}$$

$$L_5 = \frac{F_3\Xi_2}{C_1 + \Xi_1^2 + \overline{H}_z}, \tag{35}$$

Equation (30), a non-homogeneous second-order ordinary differential equation, is the governing equation for the displacement of the cylinder which is subjected to the axisymmetric thermo-electro-magneto-mechanical loading. The corresponding general solution for the homogeneous differential equation can be written as:

$$U_g = F_4 \underbrace{\chi^{\Gamma_1}}_{u_{g1}} + F_5 \underbrace{\chi^{\Gamma_2}}_{u_{g2}}, \tag{36}$$

in which F_4 and F_5 are the integration constants to be determined by the boundary conditions. Γ_1 and Γ_2 are the roots of the corresponding characteristic equation of Eq. (36) and may be evaluated from the following Eq.:

$$\Gamma_{1,2} = \frac{(1-L_1) \pm \sqrt{(L_1-1)^2 - 4L_2}}{2} \tag{37}$$

The particular solution for Eq. (30) is assumed to have the form:

$$U_p = \chi^{\Gamma_1} U_{p1} + \chi^{\Gamma_2} U_{p2}, \tag{38}$$

where

$$U_{p1} = -\int \frac{\chi^{\Gamma_2} R(\chi)}{W_p} d\chi, \tag{39}$$

$$U_{p2} = \int \frac{\chi^{\Gamma_1} R(\chi)}{W_p} d\chi, \tag{40}$$

in which

$$W_p = \begin{bmatrix} U_{g1} & U_{g2} \\ (U_{g1})' & (U_{g2})' \end{bmatrix}, \tag{41}$$

$$R(\chi) = -L_3\chi - L_4\chi \ln(\chi) - L_5, \tag{42}$$

Finally, the radial diszplacement is the sum of the general and particular solution as:

$$U = U_g + U_p, \tag{43}$$

By substituting U from Eq. (43) into Eq. (36) and performing the integration, Φ is obtained as:

$$\Phi = \left[\int \left\{ -\frac{F_3}{\chi} + \Xi_1 \left(\frac{dU}{d\chi} - \alpha_{rr} \left(F_1 \ln(\chi) + F_2 \right) \right) + \Xi_2 \left(\frac{U}{\chi} - \alpha_{\theta\theta} \left(F_1 \ln(\chi) + F_2 \right) \right) \right\} d\chi \right] + F_6 . \tag{44}$$

Also, by substituting U from Eq. (43) into Eqs. (27), (28), and (29) the expressions for the radial, circumferential and axial stresses can be obtained. The boundary conditions at the inner and outer surfaces for each case can be written as follows:

$$\sigma_r(1) = -1, \quad \sigma_r(\chi) = 0, \quad \Phi(1) = 1, \quad \Phi(\chi) = 1, \quad T(1) = 1, \quad T(\chi) = b, \tag{45}$$

4. Numerical results and discussion

The numerical results are drawn in Figs. 2-6 which show the magnetic field effects on the variation of stress, the electric potential and the radial displacement across the thickness of the nanocomposite cylinder. The presented results are for the boundary conditions described above in Eq. (68), with aspect ratio of $b/a = 2$. The plots in these figures correspond to $T(a) = 323$ K and $T(b) = 298$ K. The piezoelectric material PVDF has been selected with the following mechanical and electrical properties [16]:

Table 1. Mechanical and electrical properties for PVDF

Properties	PVDF	
c_{11}	238.24	(GPa)
c_{12}	3.98	(GPa)
c_{22}	23.6	(GPa)
e_{11}	-0.135	(C/m^2)
e_{12}	-0.145	(C/m^2)
e_{11}	1.1e-8	(C^2/Nm^2)
α_r	7.1e-5	(1/K)
α_θ	7.1e-5	(1/K)

The magnetic permittivity of CNTs is selected as $\mu = 4\pi \times 10^{-7} N/A^2$, and the magnetic field intensity is $H_z = 1 \times 10^8 A/m$.

The magnetic field effects on the graphs of the radial stress, the circumferential stress, the axial stress, the effective stress, the electric potential, and the radial displacement along the radial direction are shown in Figs. 2-6, respectively, for the proposed boundary condition. These figures indicate clearly that the magnetic field has a major effect on the electro-thermo-elastic stresses, the radial displacement, and the electric potential. Fig. 2 depicts the distribution of the radial stress along the radius. As can be seen, the radial stresses at the internal and external surfaces of the cylinder satisfy the given boundary conditions. Moreover, the existence of the magnetic field decreases the radial stress.

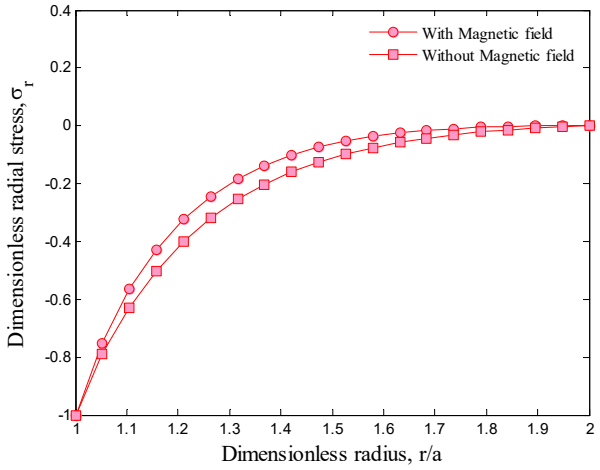

Fig. 2. Magnetic field effects on the redial stress

The distributions of the hoop and the effective stresses are displayed in Figs. 3 and 4, where the hoop and the effective stresses are monotonically changed from the inner to the outer radius. Furthermore, the hoop and the effective stresses decrease in the existence of the magnetic field. It is due to the fact that in the existence of the magnetic field, the stiffness of the cylinder increases.

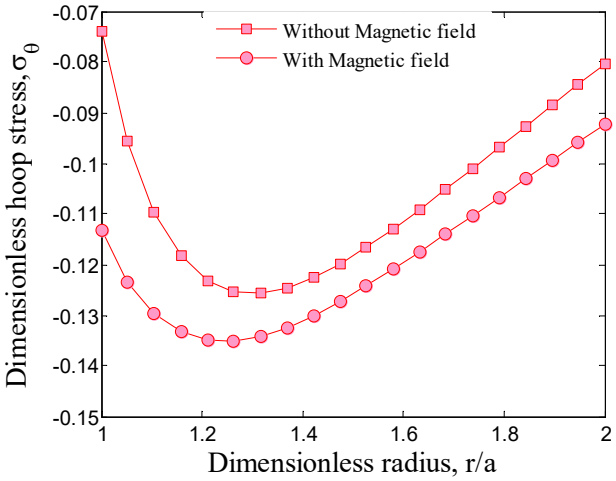

Fig. 3. Magnetic field effects on the hoop stress

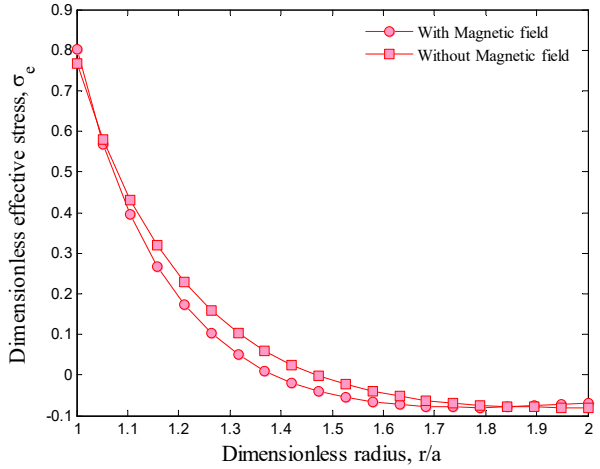

Fig. 4. Magnetic field effects on the effective stress

Fig. 5 shows the electric potential through the thickness of the nanocomposite cylinder. It can be seen from this figure that the electric potential satisfies the boundary conditions and increases in the existence of the magnetic field.

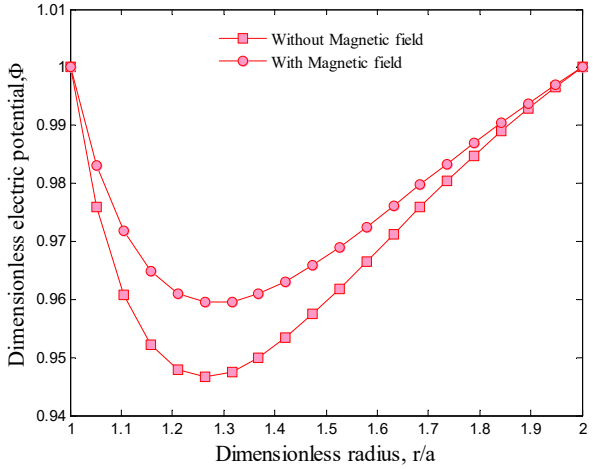

Fig. 5. Magnetic field effects on the electric potential

The variations of the radial displacement along the radius are demonstrated in Fig. 6, which indicates that the radial displacement decreases in the existence of the magnetic field, and its maximum value occurs at the outer radius, since in the existence of the magnetic field, the stability of the structure increases, and hence, the radial displacement decreases.

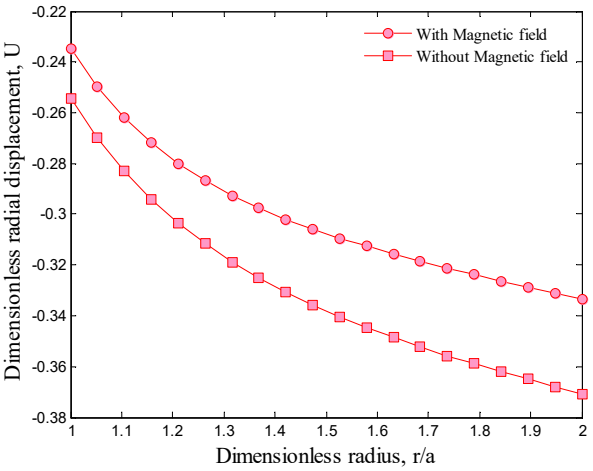

Fig. 6. Magnetic field effects on the radial displacement

5. Conclusions

The magnetic field effects on the electro-magneto-thermo-mechanical analysis of the piezoelectric cylinders reinforced with CNTs were the main contributions of this work. The equivalent material properties of the system were obtained using the Mori-Tanaka model. The coupled governing equation was derived based on the Maxwell and the equilibrium equations. In order to obtain the stresses, the electric potential, and the radial displacement distributions an analytical method was applied. The results indicated that in the existence of the magnetic field, the stresses reduce. Furthermore, the tensile hoop and the effective stresses were monotonically changed from the inner to the outer radius.

References

[1] Ghorbanpour, A., Golabi, S. and Saadatfar, M., "Stress and electric potential fields in piezoelectric smart spheres", Journal of Mechanical Science and Technology, Vol. 20, pp. 1920-1933, 2006.
[2] Saadatfar, M. and Razavi, A.S., "Piezoelectric hollow cylinder with thermal gradient", Journal of Mechanical Science and Technology, Vol. 23, pp. 45-53, 2009.
[3] Galic, D. and Horgan, C.O., "The stress response of radially polarized rotating piezoelectric cylinders", Journal of Appllied Mechanics, Vol. 66, pp. 257-272, 2002.
[4] Chen, Y., Shi, Z.F., "Analysis of a functionally graded piezothermoelatic hollow cylinder", Journal of Zhejiang University SCIENCE A, Vol. 6, pp. 956–61, 2005.

[5] Babaei, M.H. and Chen, Z.T. “Analytical solution for the electromechanical behaviour of a rotating functionally graded piezoelectric hollow shaft”, Archive of Appllied Mechanics, Vol. 78, pp. 489–500, 2008.
[6] Khoshgoftar, M.J., Ghorbanpour Arani, A. and Arefi, M. “Thermoelastic analysis of a thick walled cylinder made of functionally graded piezoelectric material”, Smart Materials and Structures, Vol. 18, pp. 115007 (8pp), 2009.
[7] Ray, M.C. and Reddy,J.N. “Active control of laminated cylindrical shells using piezoelectric fiber reinforced composites”, Composite Science and Technology, Vol. 65, pp. 1226–1236, 2005.
[8] Bohm, H.j. and Nogales, S. “Mori–Tanaka models for the thermal conductivity of composites with interfacial resistance and particle size distributions”, Composite Science and Technology, Vol. 68, pp. 1181–1187, 2008.
[9] Tan, P. and Tong, L. “Micro-electromechanics models for piezoelectric-fiber-reinforced composite materials”, Composite Science and Technology, Vol. 61, pp. 759–769, 2001.
[10] Loghman, A. and Cheraghbak, A. “Agglomeration effects on electro-magneto-thermo elastic behavior of nano-composite piezoelectric cylinder”, Polymer Composites, 2016, DOI: 10.1002/pc.24104.
[11] Mori, T. and Tanaka, K., “Average Stress in Matrix and Average Elastic Energy of Materials with Misfitting Inclusions”, Acta Metallurgica et Materialia, Vol. 21, pp. 571- 574, 1973.
[12] Shi, D.L. and Feng, X.Q.و T“he Effect of Nanotube Waviness and Agglomeration on the elastic Property of Carbon Nanotube-Reinforced Composties”, Journal of Engineering Materials and Technology ASME, Vol. 126, pp. 250-270, 2004.
[13] Ghorbanpour Arani, A., Kolahchi, R. and Mosallaie Barzoki, A.A. “Effect of material in-homogeneity on electromechanical behaviors of functionally graded piezoelectric rotating shaft”, Applied Mathematical Modelling, Vol. 135, pp. 2771–2789, 2011.
[14] Ghorbanpour Arani, A., Loghman, A., Abdollahitaheri, M. and Atabakhshian, V. “Electrothermomechanical behaviour of a radially polarized functionally graded piezoelectric cylinder”, Journal of Mechanics of Materials and Structures, Vol. 6, pp. 869–882, 2011.
[15] Dai, H.L., Hong, H., Fu, Y. and Xiao, M. “Analytical solution for electromagneto thermoelastic behaviours of a Functionally Graded Piezoelectric Hollow Cylinder”, Applied Mathematical Modeling, Vol. 34, pp. 343-357, 2010.
[16] Ghorbanpour Arani, A., Mosallaie Barzoki, A.A., Kolahchi, R., Mozdianfard, M.R. and Loghman, A. “Semi-analytical solution of time-dependent electro-thermo-mechanical creep for radially polarized piezoelectric cylinder”, Computers and Structures, Vol. 89, pp. 1494–1502, 2011.